



Biobased high-performance polyesters: Synthesis and thermal properties of poly(isoidide furanoate) and co-polyesters

Willem Vogelzang, Rutger J. I. Knoop, Daan S. van Es, Rolf Blaauw, Evelien Maaskant*

Wageningen Food and Biobased Research, Wageningen University and Research, P.O. Box 17, 6700 AA Wageningen, The Netherlands

ARTICLE INFO

Keywords:

Isohexide
Isoidide
2,5-furandicarboxylic acid
Biobased polyester
High-performance
Solid-state post-condensation

ABSTRACT

A fully biobased high-performance polyester was prepared by the sequential melt polymerization and solid-state post-condensation of the symmetrical 1,4:3,6-dianhydrohexitol isoidide and dimethyl 2,5-furandicarboxylate (FDME). The thermal properties of the resulting poly(isoidide furanoate) were well within the “high-performance” range with a glass transition- and melting temperature of approx. 165 and 280 °C, respectively. Since such a high melting temperature does not allow for conventional melt processing without thermal degradation of the polymer, various C2-C4 diol comonomers were incorporated in an attempt to create semi-crystalline co-polyesters with a high-glass-transition-temperature and sufficiently low melting point. It was found that semi-crystalline co-polyesters could be obtained with either low (3–5 mol%) or high (80–95 mol%) isoidide contents. All semi-crystalline co-polyesters with low diol comonomer contents (≤ 20 mol%) had still glass transition temperatures ≥ 118 °C despite having low molecular weights. Co-polyesters with a high diol comonomer content had lower melting points than the PiIF homopolymer, as well as a significantly lower glass transition temperature. The molecular weight of the PiIF homopolymer and a semicrystalline poly(ethylene-co-isoidide furanoate) co-polyester could be significantly enhanced by solid-state post-condensation. Thus, poly(isoidide furanoates) are an interesting class of new fully biobased polyesters that has potential in high-performance applications.

1. Introduction

The increasingly more observable effects of global climate change due to anthropogenic greenhouse gas emissions are supporting the need for several transitions with the aim to eliminate the use of non-renewable energy and materials feedstocks. While renewable energy can be generated via a myriad of different technologies, such solar-, wind-, and hydropower, renewable carbon for the production of chemicals and materials only has three sources; *i.e.*, biomass, carbon dioxide and organic recycle streams [1]. Biomass, and especially residual biomass obtained from primary production for *e.g.*, food production or forestry, is a valuable, concentrated renewable carbon feedstock. The majority of terrestrial plant biomass consists of polysaccharides (*e.g.*, cellulose, hemicellulose, starch, pectins, chitin) and carbohydrates (sucrose, glycerol, etc.) [2]. Hence using carbohydrate-based biomass to produce functional chemicals, platform chemicals and materials is a logical choice based on widespread availability. Unfortunately, most of the native polysaccharides and carbohydrates are unsuitable direct substitutes for current petrochemical derived materials and building

blocks, especially those aimed at demanding applications, such as high temperature resistance, high strength, and high barrier properties. Many of these requirements are currently met by using rigid aromatic based building blocks, such as terephthalic acid (used in, for example, poly(ethylene terephthalate) (PET), poly(butylene terephthalate) (PBT), aramids), isophthalic acid (PET, aramids) or bisphenols (polycarbonate, epoxy resins). While many building blocks for carbon-based materials can already routinely be made from carbohydrate biomass (*e.g.*, glycols, aliphatic diacids), biobased aromatic building blocks are still in their early stages of development due to a combination of factors (cost competition from fossil-based incumbents being a major one). An alternative to the use of actual aromatics can be found in carbohydrate derived furanics, with a focus on furan-2,5-dicarboxylic acid (FDCA). Although already reported over 150 years ago, this hetero-aromatic diacid has become the subject of increasing research efforts due to the relatively high selectivity with which it can be made from carbohydrates [3,4]. FDCA has been proposed as viable alternative for *e.g.*, terephthalic acid, isophthalic acid, and phthalic acid in a multitude of applications, ranging from engineering thermoplastics to plasticisers and coating

* Corresponding author.

E-mail address: evelien.maaskant@wur.nl (E. Maaskant).

<https://doi.org/10.1016/j.eurpolymj.2023.112516>

Received 18 August 2023; Received in revised form 5 October 2023; Accepted 13 October 2023

Available online 15 October 2023

0014-3057/© 2023 The Authors. Published by Elsevier Ltd. This is an open access article under the CC BY license (<http://creativecommons.org/licenses/by/4.0/>).

resins, and beyond [5–7]. Although recently some concerns were raised about the photo stability of FDCA based materials [8,9], many of the advocated unique properties, such as exceptional gas barrier properties of poly(ethylene furanoate) (PEF), warrant further development [10–12]. PEF is a commercially highly interesting fully biobased, and recyclable polyester that can replace PET in a variety of packaging applications. Although PEF has thermal properties that are close to those of PET, there is still a need for (bio)renewable materials that are more comparable to true engineering plastics like bisphenol-based polycarbonate. This requires increasing thermal properties like the glass transition temperature (T_g) by the incorporation of rigid building blocks (such as a diacid and diols) that limit polymer chain movement.

An interesting class of carbohydrate-derived rigid diols are the so-called isohexides (or 1,4:3,6-dianhydrohexitols), for which three stereoisomers exist that differ in the orientation of their OH groups: isomannide, isosorbide, and isoidide (Fig 1). The glucose-derived isosorbide is the most well-known, and most accessible isomer. Isosorbide, obtained efficiently by the acid-catalysed cyclodehydration of sorbitol (obtained by glucose hydrogenation), was first reported more than 95 years ago [13]. It is a commercial product that is used in various applications ranging from pharmaceuticals, to plasticisers, to plastics. Isosorbide is non-toxic and diesters or polyesters thereof are often reported to be biodegradable [14–16], making it an ideal renewable polymer building block.

Incorporation of this rigid diol into a broad range of polymers, including PET and PEF, was shown to result in increases in T_g [17]. Despite these favourable effects, there are two main drawbacks to the use of isosorbide in polycondensations. The first is the necessity to use harsh polymerization conditions to compensate for the low reactivity of the secondary hydroxyl groups. The *endo*-hydroxyl group in particular is

not very reactive. This leads to thermal degradation with concomitant strong discoloration and low polymer weights [18]. The same is observed with isomannide (derived from mannitol), which has both hydroxyl groups in an unfavourable *endo*-orientation [19,20].

The second drawback of isosorbide as a (co-)monomer is that, unlike isomannide and isoidide, it lacks symmetry and, as a result, polymers derived from it are often amorphous [21–23]. This precludes the use of industrially applied methods to increase polymer weights such as solid-state post-condensation (SSPC), which is effective only when the polymer is semi-crystalline [24,25].

For these reasons, it is expected that isoidide, being both symmetrical and having two *exo*-hydroxyls, offers the best potential among the three isohexide isomers as a (co-)monomer that may yield semi-crystalline polyesters with a high T_g . Although the limited availability of isoidide (due to scarceness of its parent hexose idose) has precluded extensive study of it in polycondensation reactions, the available literature seems to support this hypothesis. Thiem *et al.* were the first to report on polyesters based on isohexides, including isoidide. Isoidide was polymerized with terephthalic acid dichloride resulting in a low molecular weight ($M_n = 3.8$ kDa) semi-crystalline polyester with a melting temperature (T_m) of 192 °C [26,27]. In a similar fashion, Storbeck and Ballauff polymerized isohexides, including isoidide, with 2,5-furandicarbonyl dichloride resulting in a high molecular weight polyester ($M_n = 21$ kDa) with a T_g of 196 °C, yet no mention was made of semi-crystalline character [28]. More recently, Gomes *et al.* reported on the synthesis of poly(isoidide 2,5-furanoate) via solution polymerization of isoidide with 2,5-furandicarbonyl dichloride, however they only obtained an M_n of 5.7 kDa [29].

Note that while solution polymerization can be applied on industrial scale, it is mostly limited to high value specialty polymers, such as

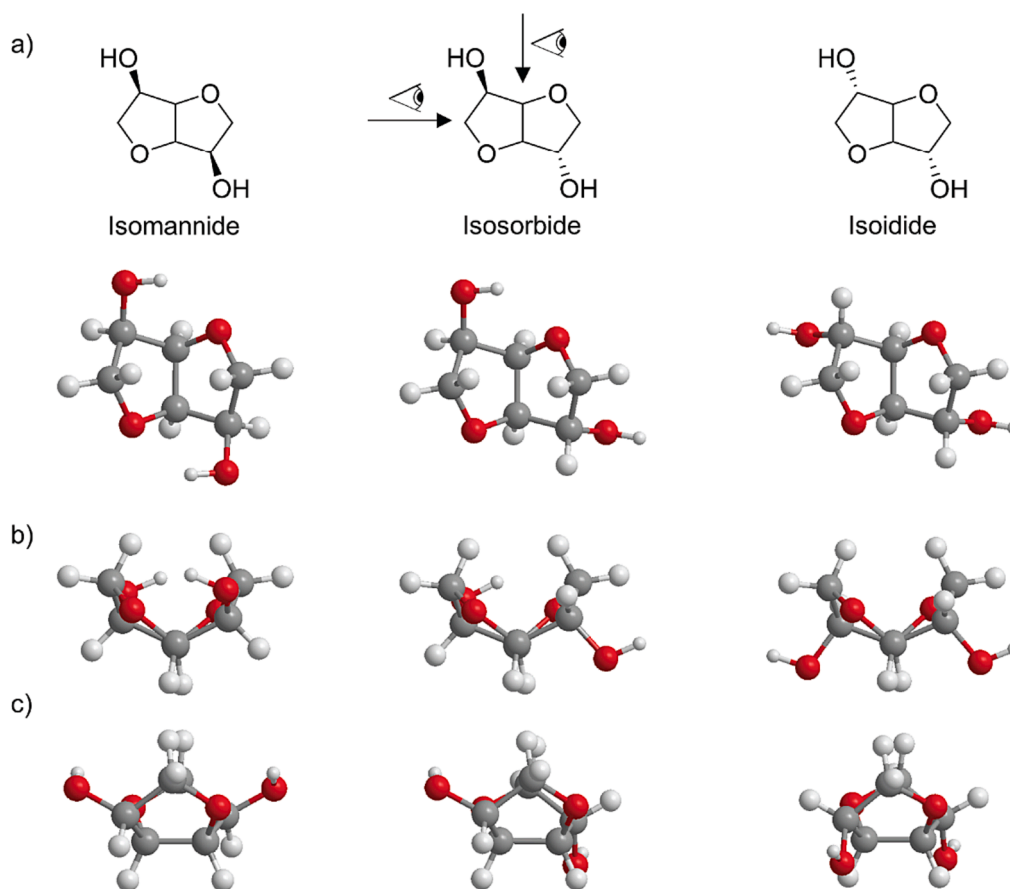


Fig. 1. Three isohexide isomers; a) 2D and 3D molecular structures; b) 3D-structures viewed from vertical axis; c) 3D-structures viewed from horizontal axis. All 3D-structures were obtained by DFT calculations; a detailed description is given in the supporting information.

polyaramids, polyether ether ketone (PEEK) or phosgene based polycarbonates [30–32]. For high T_g biobased engineering plastics with properties similar to that of BPA-polycarbonate, common industrial processes like melt polymerization followed by SSPC are highly preferred not only from a cost point of view, but also from a sustainability perspective.

Recently, industrially feasible methods were published for the catalytic epimerisation of commercially available isosorbide to a mixture of all three isohexide isomers, with isoidide being the major isomer. Using industrially applied separation techniques, high purity, resin-grade isoidide can now be obtained [33,34]. This has opened opportunities to study the use of this isomer in polycondensations and to evaluate its effect on the properties of the resulting polyesters.

Hence, here we report on the synthesis and properties of fully renewable polyesters derived from isoidide (ii) and dimethyl furan-2,5-dicarboxylate (furanate dimethyl ester, FDME) via industrially relevant sequential melt polymerization-SSPC. The prepared polymers include both poly(isoidide furanoate) (PiIF) homopolymer, as well as PiIF copolyesters that contain an C2-C4 diol comonomer (ethylene glycol, 1,3-propanediol, 1,4-butanediol or 2,3-butanediol). The aim of this study was to verify the expected benefits of ii over isosorbide in terms of reactivity in polycondensations, processability (effectiveness of SSPC) and polymer properties when preparing polyfuranates.

2. Experimental

2.1. Materials

Ethylene glycol (EG, anhydrous, 99.8%), 1,4-butanediol (1,4-BDO, 99%), 2,3-butanediol (2,3-BDO, 98%), *o*-xylene (>99%), titanium(IV) isopropoxide ($\text{Ti}(\text{iOPr})_2$, 97%), trifluoroacetic acid (TFA, 99%), chloroform-*d* (CDCl_3), trifluoroacetic acid-*d*₁ (TFA-*d*₁), and potassium trifluoroacetate (98%) were obtained from Sigma-Aldrich (The Netherlands). 1,3-propanediol (1,3-PDO, 99%) was obtained from Alfa Aesar (the Netherlands). 1,1,1,3,3,3-hexafluoro-2-propanol (HFIP) was obtained from Fluorochem (United Kingdom). Dimethyl 2,5-furandicarboxylate (FDME) and isoidide (ii) were supplied by Archer Daniels Midland Company (United States of America). All chemicals were used as received.

2.2. General melt polycondensation procedure

A pre-dried 100 mL three-necked round bottom flask equipped with a magnetic drive overhead mechanical stirrer (Büchi AG bmd075), nitrogen gas inlet, and Claisen distillation head with Liebig condenser was charged with dimethyl 2,5-furandicarboxylate (7–15 g, 38–81 mmol) and diols (1.3 mol equivalent). The reaction flask was evacuated and refilled with nitrogen gas three times. The reaction was performed in two stages. During the first stage, the transesterification stage, the reaction mixture was heated under nitrogen atmosphere to 160 °C (externally measured). When the reaction mixture is fully molten, the catalyst titanium(IV)isopropoxide (0.02 mol% to the dimethyl ester) in 2 mL *o*-xylene was added. The temperature was increased to 165 °C, and the mixture was stirred for 16 h. During this period methanol and *o*-xylene were collected in the receiving flask. The temperature was further increased to 220 °C, and the mixture was stirred for another 4 h. After completion of the first stage, the second stage of the polymerization was started by gradually applying a vacuum (reaching eventually 0.01–0.02 mbar). The mixture was stirred for another 3 h, and then cooled to room temperature under a nitrogen atmosphere. The crude polymer was removed from the round bottom flask by pouring liquid nitrogen in the flask to freeze the polymer, followed by breaking the round bottom flask.

All polyesters were obtained as brittle solids. The colour of the polymer varied from pale yellow (low isoidide content) to dark brown (high isoidide content).

2.3. Purification of the polyesters

Part of the polymers were purified by dissolving the polymer in a 6:1 chloroform/TFA mixture (10 wt% solution) and precipitating in excess methanol. The precipitated polymer was collected by filtration and dried *in vacuo* at 40 °C.

2.4. Solid state post condensation (SSPC)

Reactor grade polymers were used directly as they still contain catalyst. Precipitated polymers were dissolved in HFIP (10 wt% solution) together with titanium(IV)isopropoxide (0.02 mol% based on molar mass of repeating unit). Evaporation of HFIP using a rotary evaporator resulted in a semi-crystalline polymer which was used without further modification for the SSPC.

Dried polymer (100 mg – 5 g) was grinded to a powder using a mortar and pestle and transferred into a baffled drying flask (Büchi). The tube was closed with a fritted glass tube and the assembly was installed in a Büchi B-585 Kugelrohr oven. The system was evacuated and refilled with nitrogen gas three times, high vacuum (0.01–0.02 mbar) was applied, and the polymer was heated to the specified time and temperature under constant stirring (25 rpm). After the reaction was complete, the mixture was cooled to room temperature under nitrogen atmosphere.

2.5. Characterization

¹H NMR (400.17 MHz) & ¹³C NMR (100.62 MHz) spectra were recorded on a Bruker Avance II spectrometer at 298 K. The used solvent was a 6:1 mixture of deuterated chloroform and trifluoroacetic acid (6:1 CDCl_3 :TFA-*d*). All spectra were internally referenced to the chloroform signal ($\delta = 7.26$ ppm).

Size exclusion chromatography (SEC) measurements were performed using a Viscotek HP-SEC system (Malvern Instruments, Malvern, United Kingdom), equipped with a VE-2001 GPCmax pump and auto sampler, a TDA305 Triple Detector Ar-ray (Right Angle Light Scattering (RALS) + Low Angle Light Scattering (LALS), Refractive Index (RI) Detector and Viscometer), and a 2X GPC column PSS PFG analytical linear M and guard column, molecular range ~ 250—2.5·10⁶ Da (PMMA in HFIP). Molecular weights were calculated with OmniSEC™ (Version 4.6) software. Hexafluoro isopropanol (HFIP) containing 0.02 M potassium trifluoroacetate was used as the eluent with a flow rate of 0.7 mL/minute. Calibration of the measurements was done with PMMA standards (Easy vial PMMA standards from Agilent Technologies, Inc., Santa Clara, CA).

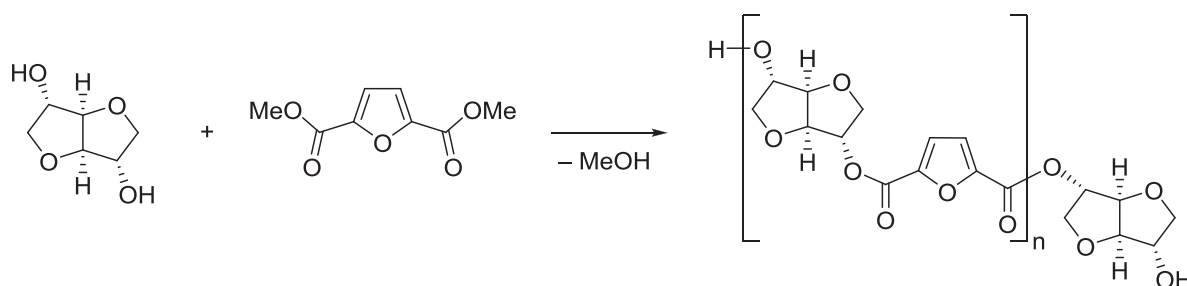
Differential scanning calorimetry (DSC) analysis was carried out with a PerkinElmer DSC 8000 with autosampler. RVS pans sealed with a rubber ring were used. An empty sealed pan was used as blank (reference) measurement. Calibration was done with indium as reference material. Samples were heated from 0 to 220–300 °C with a heating rate of 10 °C/min and a cooling rate of 100 °C/min or 10 °C/min. The results were evaluated with Perkin Elmer Pyris software.

Thermogravimetric analysis (TGA) was performed using a PerkinElmer STA 6000. The samples were heated from 30 to 600 °C with a heating rate of 10 °C/min under a nitrogen flow of 20 mL/min.

3. Results and discussion

3.1. Poly(isoidide furanoate)

Poly(isoidide furanoate) (PiIF), see Scheme 1, was prepared by the two-step melt polycondensation of FDME and ii. During the high vacuum phase at 220 °C, the polymer solidified and therefore, the polymerization was stopped immediately after solidification. ¹H NMR analysis of the crude polymer confirmed the formation of PiIF as shown in Fig. 2a (the ¹H- and ¹³C NMR spectra of PiIF and its monomers and



Scheme 1. The synthesis of PiIF by the melt polycondensation of dimethyl 2,5-furandicarboxylate (FDME) and isosorbide (ii).

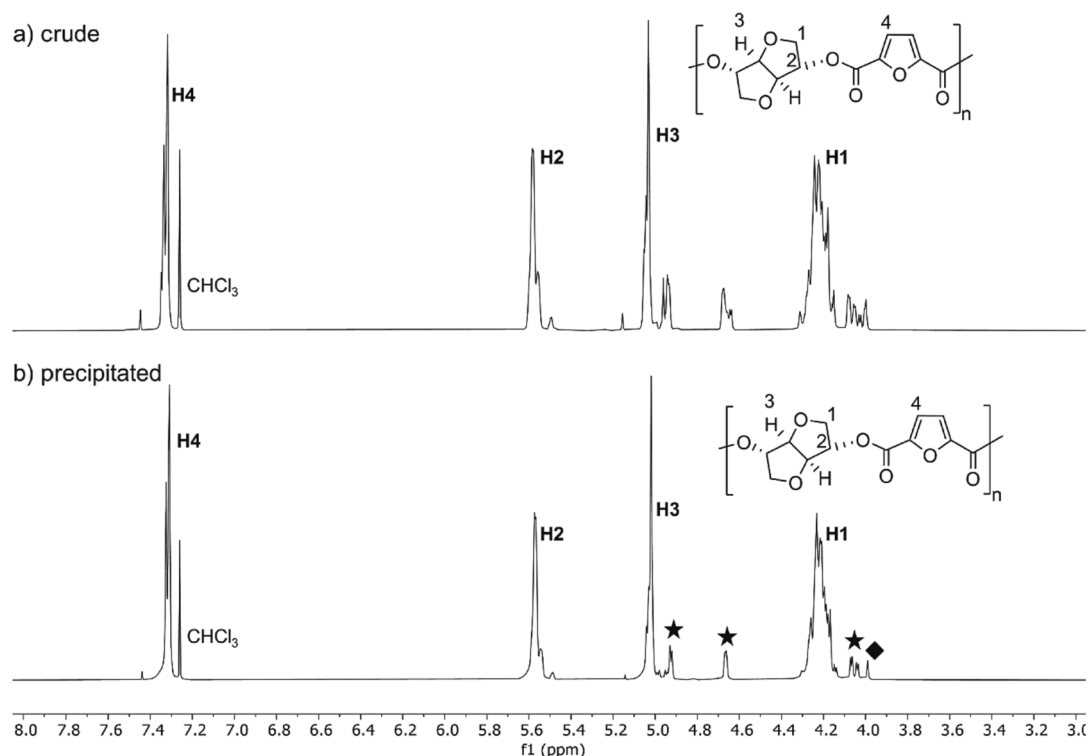


Fig. 2. ¹H NMR spectra of (a) crude, and (b) precipitated PiIF. The isosorbide end-groups are marked with a star and the FDME end-group (–OCH₃) is marked with a diamond. See Figures S2–S7 for the full range ¹H NMR spectra and ¹H- and ¹³C NMR spectra of PiIF, its monomers and other model compounds.

other model compounds are given in Figures S2–S7). Although the polymer was found to be mainly terminated with isosorbide end-groups (signals at 4.93, 4.66 and 4.05 ppm), a minor signal of methyl-ester end-groups originating from FDME was observed (3.99 ppm). The molecular weight of the crude PiIF was determined with size exclusion

chromatography (SEC). Due to the preliminary solidification of the PiIF during the melt polycondensation, the molecular weight was found to be relatively low with a number averaged molecular weight (M_n) of 1.5 kDa and a polymer dispersity index (\mathcal{D}) of 2.8. Despite this low molecular weight, the polymer was found to already have a glass transition

Table 1

Molecular weight and thermal properties of PiIF before and after SSPC. Reactor grade poly(isosorbide furanoate) (PiSF) was synthesized as a reference. Note that a cooling rate of 100 °C/min was used in all DSC measurements unless mentioned otherwise. n.o.: not observed, n.d.: not determined.

Entry	T_{SSPC} (°C)	Time (h)	M_n^a (kDa)	M_w^a (kDa)	\mathcal{D}^b	DSC 1st heating			DSC 2nd heating		
						T_g (°C)	T_m (°C)	ΔH (J/g)	T_g (°C)	T_m (°C)	ΔH (J/g)
1a-reactor grade	–	–	1.5	4.0	2.8	96	241	30	112	n.o.	n.o.
1b-reactor grade	–	–	1.5	4.0	2.8	94	240	27	109 ^c	n.o. ^c	n.o. ^c
1-precipitated	–	–	2.9	5.0	1.7	87	230	10	89	n.o.	n.o.
2	230	4	14.2	30.7	2.2	n.o.	274	36	159	n.o.	n.o.
3	230	16	19.8	44.1	2.2	n.o.	281	41	170	n.o.	n.o.
4	230	40	17.7	43.9	2.5	n.o.	274	35	164	n.o.	n.o.
5	240	2	17.9	45.3	2.5	n.o.	274	36	168	n.o.	n.o.
6	240	16	20.9	55.3	2.6	n.o.	284	42	174	n.o.	n.o.
PiSF-reactor grade	–	–	2.0	4.6	2.2	101	n.o.	n.o.	n.d.	n.d.	n.d.

^a Obtained from triple detection size exclusion chromatography (SEC), ^bPolydispersity index, ^cAfter cooling with 10 °C/min.

temperature (T_g) of 111 °C, see Table 1. This T_g matches well with that of other high-performance polyesters such as poly(1,4-cyclohexylenedimethylene-co-2,2,4,4-tetramethyl-1,3-cyclobutylene terephthalate) [35,36] (T_g 110–120 °C, commercialized by Eastman Chemical Company under the tradename Tritan) and poly(ethylene-co-1,4-cyclohexylenedimethylene-co-isosorbide terephthalate) [37,38] (T_g 90–110 °C, commercialized by SK Chemicals under the tradename ECOZEN) of which the latter two polyesters have significantly higher molecular weights than the PiIF in this work. Precipitation of the crude polymer resulted in removal of low-molecular weight oligomers (see Fig. 2b for ^1H NMR spectra after precipitation) and, consequently, an almost two-fold increase in M_n (2.9 kDa obtained with SEC) and a significant decrease in \bar{D} (1.7). The M_n was also calculated using end-group analysis by ^1H NMR, which resulted in an M_n of 2.0 kDa. A lower value by end-group analysis as compared to SEC is also reported for other polyesters by Little et al. [39].

In order to prevent the solidification of the PiIF polymer during melt polycondensation, several other reaction conditions were screened. For example, the polymerization temperature was increased from 220 to 240 or 260 °C. Nevertheless, independent of the temperature profile chosen, the PiIF polymer solidified during the high-vacuum phase resulting in low molecular weight oligomers ($M_n < 4$ kDa, data not shown). This solidification is likely caused by the preliminary crystallization of the polymer chains, and indeed, differential scanning calorimetry (DSC) of the crude PiIF (Table 1 entry 1a) showed a melting transition in the first heating curve with a maximum at 241 °C, indicating that the PiIF was semi-crystalline (see also Fig. 3 for the DSC curves). This is in contrast with the closely related poly(isosorbide furanoate) (PiSF) which is reported to be amorphous [40,41]. PiSF was also synthesized as a reference in this work, and was also found to be fully amorphous with a T_g of 101 °C.

The molecular weight of semi-crystalline polymers can be increased by the industrially commonly used method SSPC [24,42]. In contrast to PiSF, the semi-crystalline nature of PiIF allowed for SSPC. Table 1 shows the molecular weights and thermal properties of PiIF after applying several SSPC conditions. First, an SSPC temperature of 230 °C was used. Already after 4 h a significant increase in molecular weight was observed reaching an M_n of 14.2 kDa. Extending the reaction time to 16 h resulted in a slightly higher molecular weight ($M_n = 19.8$ kDa). Further extending the reaction time to 40 h led to no significant changes in molecular weight, i.e. the SSPC reaction stopped, probably caused by

a reduction in the availability of end-groups in the amorphous domains as the SSPC reaction proceeds. This phenomenon is common in the SSPC of polyesters, and similar behaviour has been reported for, for example, poly(ethylene terephthalate) (PET) [25,43], poly(ethylene furanoate) (PEF) [44,45], poly(trimethylene terephthalate) (PTT) [46], poly(trimethylene furanoate) (PTF/PPF) and poly(butylene furanoate) (PBF) [47]. In addition, one could speculate that given the high rigidity of the backbone of PiIF it is likely that the amorphous regions consist mainly of rigid amorphous phase, in which the end-groups have a significantly lower mobility compared to the mobile amorphous phase. Also the secondary diol isosorbide is less reactive than commonly used primary diols. Furthermore, the crystallinity of PiIF increases during SSPC, given the increase in ΔH_m , and thus the amount of amorphous phase decreased over time. However, a more detailed study on the SSPC kinetics was out of scope for this work.

Although increasing the SSPC time to 40 h did not significantly affect the molecular weight, it did result in an increase in \bar{D} . This can be explained by thermal degradation of the polymer, or by the occurrence of side reactions, upon prolonged exposure to high temperatures. Due to the dark brown colour of the crude PiIF, no visual signs of degradation could be observed after SSPC. Increasing the SSPC temperature to 240 °C accelerated the initial molecular weight build-up; an M_n of 17.9 kDa was already observed after 2 h (Table 1, entry 5). However, after 16 h (Table 1, entry 6) the increase in molecular weight clearly slowed down resulting in only a minor increase in M_n (20.9 kDa). In addition, a higher SSPC temperature resulted in a higher \bar{D} after the same reaction time (2.6 after 16 h at 240 °C versus 2.2 after 16 h at 230 °C) suggesting that this higher SSPC temperature results in more undesired side reactions. Unfortunately, it was not possible to obtain unambiguous spectroscopic evidence of changes in the chemical structure of PiIF after SSPC. However, like other alcohols, isohexides and their (poly)esters are reported to be susceptible to β -elimination reactions (Scheme 2a) [48,49]. Already in 1956 it was reported that isosorbide or its diacetate generate the corresponding diene under pyrolytic conditions [50]. Various authors have reported on the increased thermal instability of isohexides containing leaving groups (i.e. triflate, tosylate, halide) on positions 2 and/or 5, often leading to decreased yields and the formation of dark, resinified products already at ambient temperatures [51,52]. Others have reported on the intentional synthesis of anhydro isohexide derivatives, which are reactive enol-ethers (Scheme 2b) [53–57]. These enol ethers are prone to react with alcohols or carboxylic acids under acid catalysis, yielding cyclic acetals, and hence aldehydes under hydrolytic conditions [58]. Interestingly, it was also reported that in absence of hydroxyl groups, under acid catalysis isohexide enol ethers rearrange to ring opened furan derivatives [58–60]. Furan derivatives without electron withdrawing substituent are known to be highly unstable under high temperature conditions [61–63].

Recently, Yan and Wu showed that beta eliminations, as well as hydroperoxide formation on the tetrahydrofuran rings of isosorbide-based polycarbonates can lead to thermal and oxidative degradation (Scheme 2c) [64]. ^1H NMR analysis showed that, albeit at very low concentration, signals that can be ascribed to enol ethers and ring opened products are observed after prolonged thermal treatment (240 °C, 60 min). Thus, based on these literature examples, it can be concluded that the thermal degradation of PiIF observed during SSPC can be caused by multiple degradation mechanisms. Note that the observed maximum value of \bar{D} for PiIF after SSPC was 2.6, which is not indicative of, e.g., severe branching or cross-linking, and hence, most likely only minor concentrations of degradation products are formed. Furthermore, it can be expected that multiple degradation reactions occur simultaneously, and that reactive intermediate species are also formed. This results in a complex mixture of degradation products, in the case of PiIF present at low concentrations, making a detailed characterization complicated.

The increase in molecular weight inherently resulted in an increase in the T_g and T_m as well. Fig. 3 shows the DSC curves for both reactor

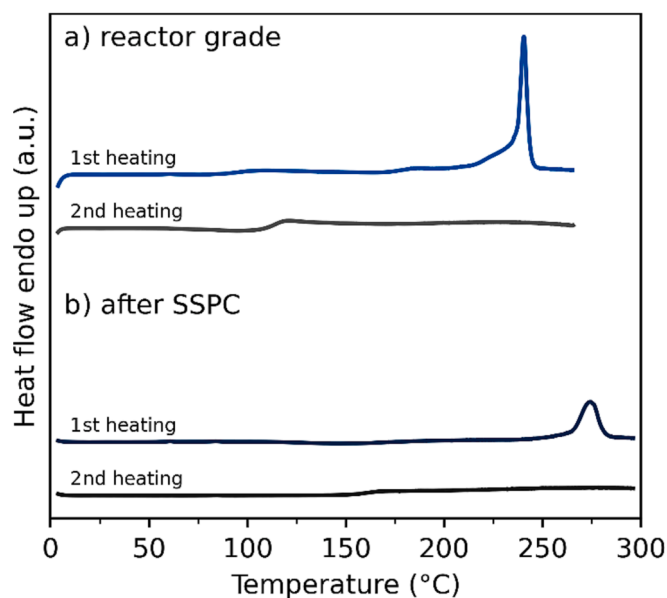
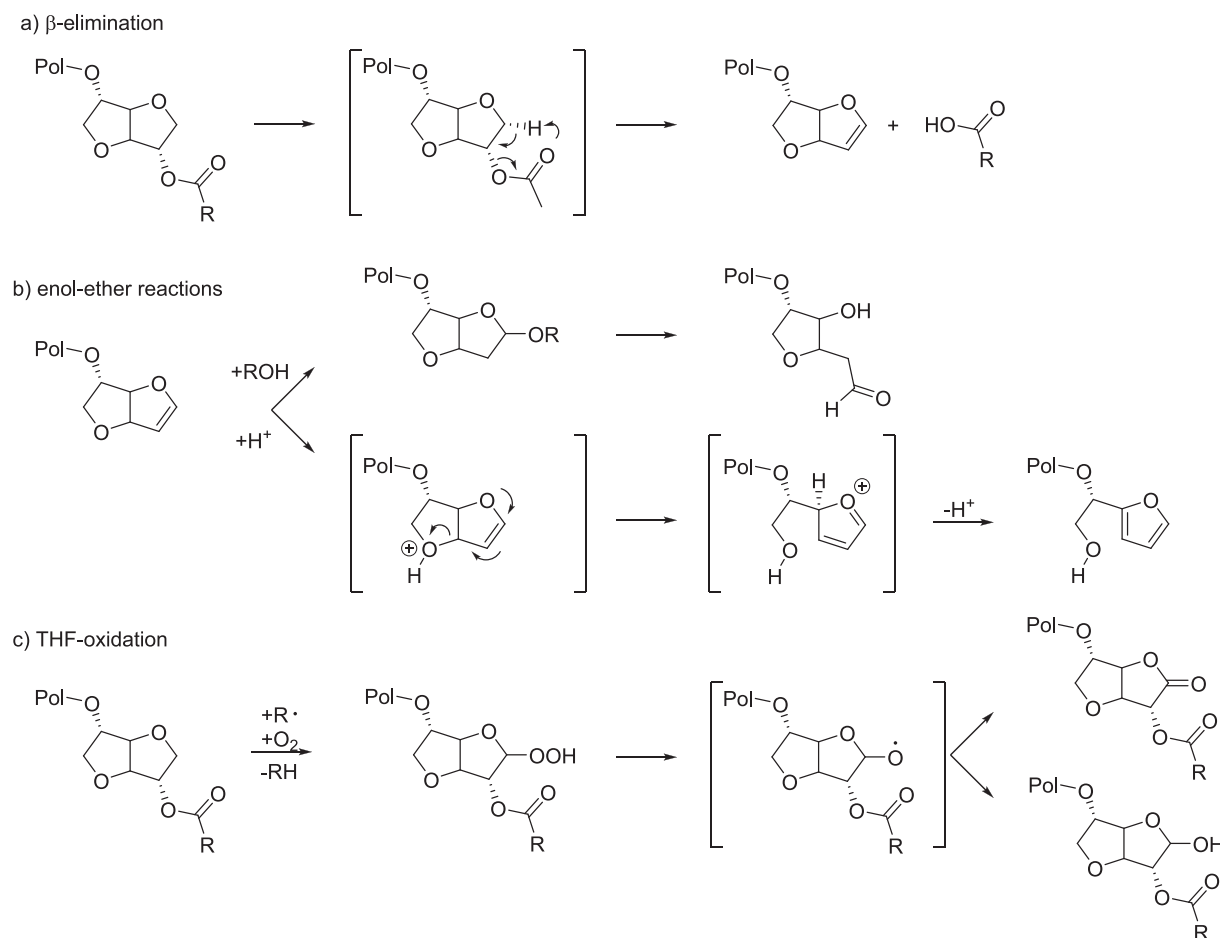


Fig. 3. Differential scanning calorimetry (DSC) curves of a) PiIF before SSPC (Table 1 entry 1a) and b) PiIF after SSPC (40 h 230 °C, Table 1 entry 4).



Scheme 2. Potential pathways for isoidide degradation by a) thermal β -elimination, b) tentative subsequent multifunctional reactive intermediates, and c) radical induced oxidation of the THF-ring; Pol = polymer residue.

grade PiIF (Table 1 entry 1a) and PiIF after SSPC (Table 1 entry 4). After unforced cooling from the melt, reactor grade PiIF shows a very broad melting transition in the first heating curve, starting already at 170 °C with a maximum at 241 °C and a melting enthalpy of 30 J/g. Apparently a small fraction of unstable crystals has been formed during the polymerization which melts and subsequently crystallizes into the more stable, and dominant, crystal structure. The second heating curve of reactor grade PiIF showed only a glass transition at 111 °C as the quench cooling (100 °C/min) applied does not allow for crystallization. Surprisingly, also when a lower cooling rate (10 °C/min) was applied, no melting transition was found in the second heating curve (Table 1 entry 1b). Thus, it can be concluded that on the time scale of a DSC measurement, PiIF was not able to crystallize, and that the crystallization kinetics are relatively slow. This can very well be explained by the rigid nature of the polymer.

As a result of the increased molecular weight after SSPC, both the glass transition and the melting transition of PiIF shifted towards higher temperatures. For example, after 40 h at 230 °C the T_g (second heating) of PiIF reached 164 °C and the T_m 274 °C (first heating, taken at the maximum) with a melting enthalpy of 35 J/g. This T_g is lower than that of PiIF reported by Storbeck and Ballauff who reported a T_g of 196 °C ($M_n = 21.5$ kDa) [28].

As melt processing of polymers is generally performed tens of degrees above the polymer's melting temperature, extremely high processing temperatures, probably exceeding 300 °C, would be required for PiIF. These high processing temperatures come at the risk of thermal degradation of the polymer during melt processing. In order to assess the thermal stability of PiIF under processing conditions, PiIF sample (not in

Table 1 due to being from another batch, M_n 7 kDa, D 2.2, SSPC conditions 16 h, 230 °C) was analysed by TGA under a nitrogen atmosphere. Fig 4a and 2b show that the onset of thermal degradation of PiIF starts at 300 °C, which is in agreement to the results found by Storbeck and Ballauff [28], and that the maximum rate of degradation is obtained at 395 °C. At this temperature only 41% of the original mass is left. Thus, especially for the higher molecular weight PiIF, it can be concluded that the processing temperature will overlap with the degradation temperature (although the degradation is not at a maximum rate yet), and that thus degradation during melt processing would be a significant problem for the application of PiIF as thermoplastic material. Like other high-performance polymers (e.g., polyaramids), PiIF can most likely be processed via solution processing, however, this is out of scope for this work.

3.2. PiIF co-polyesters

Although the PiIF polymer has a T_g well within the "high performance polymers" range, its T_m is very high and too close to the thermal degradation temperature, making melt processing almost impossible. Therefore, it was attempted to decrease the melting temperature of PiIF by adding C2-C4 diols as comonomers. This approach possibly gives co-polyesters with a high T_g while at the same time being processable in the melt without decomposition. A series of PiIF co-polyesters, PEiIF, PPiIF, P1,4-BiIF and P2,3-BiIF, was prepared by adding different ratios of either ethylene glycol (EG), 1,3-propanediol (PDO), 1,4-butanediol (1,4-BDO), or 2,3-butanediol (2,3-BDO), respectively (Scheme 3). The effect of diol comonomer on the polymers' molecular weights and thermal

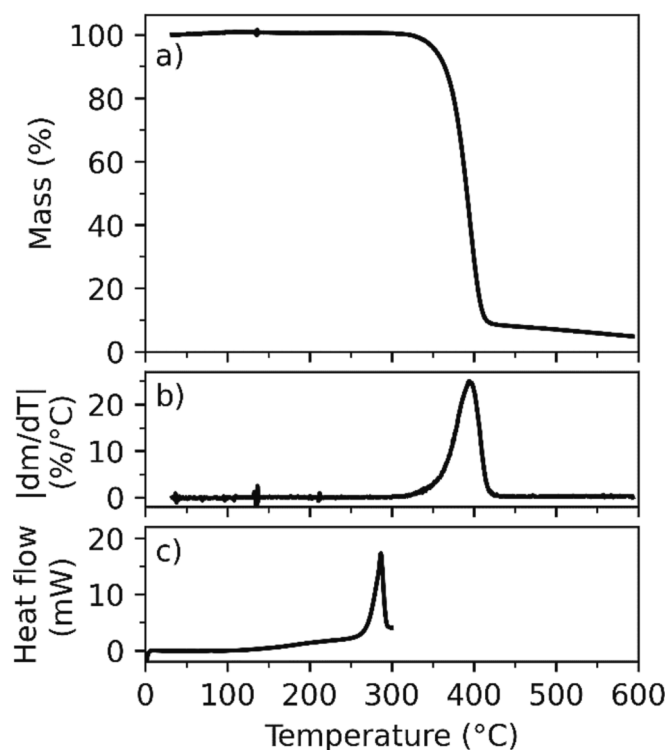
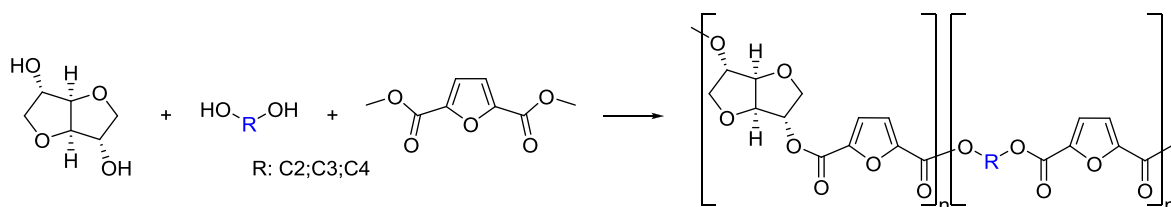


Fig. 4. a) mass loss of PiIF (M_n 7 kDa) as function of temperature after SSPC (16 h, 230 °C) measured under a nitrogen atmosphere, b) derivative mass loss of curve a) showing that the onset of thermal degradation starts around 300 °C, and c) the heat flow (endo up) obtained from the DSC first heating curve of the same PiIF sample.

properties was studied.

The structure of all PiIF co-polymers was confirmed by ^1H - and ^{13}C NMR. As an example, the ^1H NMR spectra of all 50:50 mol% iI-diol mixtures are given in Fig. 5. Based on the ^{13}C NMR spectra (see Supporting Information), the degree of randomness was calculated and was found to be 0.99–1.02 for all 50:50 mol% PiIF co-polymers except P2,3-B[50]iI[50]F, indicating a random structure [65–68]. For P2,3-B[50]iI[50]F the degree of randomness could not be calculated due to the complex splitting pattern caused by the stereoisomers of 2,3-BDO. From the ratio of integrals of the iI and methylene protons of the diol comonomer, the incorporation ratio of both diols in the polymer could be determined. The calculated incorporation ratio for all polyesters is given in Table 2. In most cases, the incorporation ratio matches relatively well with the feed ratio. Minor differences can be attributed to the error margin in the integration of the NMR signals. However, some polymer compositions show a composition drift of a couple of percentage points. Interestingly, the observed composition drift is towards a lower EG incorporation, whereas for the other diol comonomers, except 2,3-BDO, the composition drift is mainly towards a higher diol comonomer incorporation. Note that there are not enough entries for 2,3-BDO to observe a trend.

The compositional drifts towards higher incorporation of the diol



Scheme 3. Synthesis of PiIF co-polyesters using C2-C4 diols as comonomers. Note that the end-groups are not drawn.

comonomers and thus lower isoidide incorporation can be explained by the lower reactivity of isoidide, a sterically hindered secondary diol. The only exception is the co-polyester series containing EG, which shows a lower incorporation of EG than expected based on diol reactivity. Here, the relatively low boiling point of EG of 197 °C [69] close to the transesterification temperature may have led to some evaporation of EG and consequently a lower incorporation compared to isoidide. The other diol comonomers have higher boiling points (PDO 213 °C, 1,4-BDO 230 °C [69]) and hence losses by evaporation are less likely. Note that boiling point effects for these diols were also reported for fully aliphatic polyesters [70].

Also the molecular weights of all PiIF co-polyesters, directly after polycondensation, were determined using size exclusion chromatography (see Table 2). A higher concentration of iI in the feed typically results in a polyester with a lower molecular weight. This can, again, be attributed to the lower reactivity of the secondary hydroxyl groups of iI. This behaviour is in good agreement with the results obtained for co-polyesters utilizing other isohexides, such as isosorbide. An extensive overview of these co-polyesters and their properties is written by Weinland *et al.* [17]. In addition, an increase in \bar{M}_w with an increasing iI content was observed. Given the same reaction temperature and time for all co-polyesters, this increase in \bar{M}_w can be attributed solely to the increase of iI content. The colour of the polyesters varied from pale yellow (low iI content) to dark brown (high iI content). Thus, most likely the increase in \bar{M}_w and stronger discoloration are caused by side reactions involving the isoidide moiety.

The thermal properties of all co-polyesters after melt polycondensation were determined using differential scanning calorimetry, and the results are shown in Table 2. In addition, Fig. 6 shows the glass transition temperatures and, when applicable, melting temperatures of all co-polyesters as function of iI-content. The glass transition temperatures of each series of co-polyesters are in general directly proportional to the iI-content, *i.e.* a higher iI content results in a higher glass transition temperature. This behaviour can be explained by the rigid nature of the iI monomer. Interestingly, the glass transition temperature drops for some series of co-polyesters when the iI-content was above 90%. Because, as defined by the Flory-Fox equation, the T_g is dependent on molecular weight [71,72], this drop in T_g is attributed to the low molecular weight of the polyesters having high iI contents. Interestingly, the molecular weights of the co-polyesters with 5 mol% diol comonomer were in the same order of magnitude as that of PiIF, but still a higher T_g was observed for these co-polyesters. Due to the limited number of samples that showed this phenomenon, we cannot draw conclusions on the potential causes of this observation.

When plotting the melting temperature obtained from the DSC first heating curve as function of iI-content (Fig. 6b) it is obvious that polymers having an iI-content above approx. 80 mol% or below approx. 5 mol% are semi-crystalline after unforced cooling from the melt. All other co-polyesters containing isoidide were found to be completely amorphous after unforced cooling from the melt, whereas the homo-polymers PEF, PPF and P1,4BF were found to be semi-crystalline as well. The measured T_g and T_m ranges of the homo-polymers are in agreement with earlier reported data on these polymers [47,73–75]. In contrast to PEF, PPF and P1,4BF; P2,3BF was found to be fully amorphous with a T_g of 91 °C, which is in agreement with the results of Gubbels *et al.* [76]. A

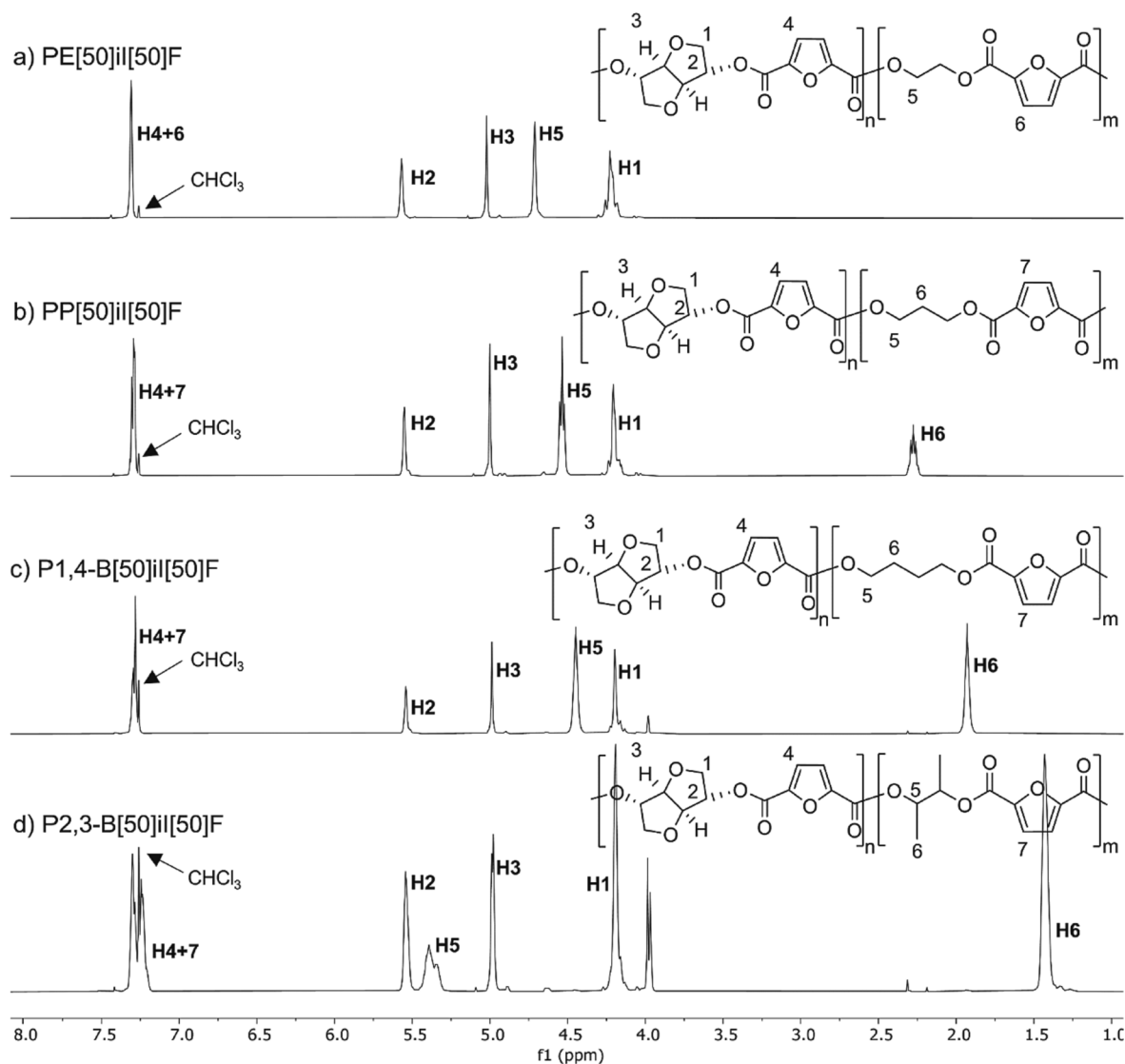


Fig. 5. ^1H NMR spectra of 50:50 mol% co-polymers of ii, FDME and the following diol comonomers: a) ethylene glycol, b) 1,3-propanediol, c) 1,4-butanediol, d) 2,3-butanediol.

more detailed, systematic study on the crystallization kinetics during annealing will be part of future work.

All homo-polymers (PEF, PPF and P1,4BF) showed also a melting transition in the DSC's second heating, whereas the crystallinity of PiIF and its co-polyesters couldn't be recovered in the second heating curve when applying the same cooling and heating rates. The only exception is PE[97]ii[3]F with 3 mol% isidide, which showed a melting transition in the second heating curve with an enthalpy of 7 J/g. This indicates that the crystallization rate of isidide-containing polyesters is very slow compared to the aliphatic homo-polymers PEF, PPF and P1,4BF. Studies on the rate of crystallization of PEF in comparison with its fossil-based analogue poly(ethylene terephthalate) (PET) showed that PEF has a lower crystallization rate than PET because the furan-flipping, needed for crystallization, is hindered [77–79]. By adding the rigid ii it is not surprising that the rate of crystallization drops even further.

Adding only a minor amount of diol comonomer (*i.e.*, co-polyesters having a high isidide content) did not result in lowering of the melting temperature. Adding moderate amounts of diol comonomer (ii content between 5 and 80 mol%) resulted in amorphous polymers after unforced cooling from the melt. This indicates that these polymers crystallize very slowly, or don't crystallize at all, and hence make them unsuitable for SSPC. However, adding just a minor amount of isidide to

PEF (PE[97]ii[3]F) resulted in a semi-crystalline polymer with a slightly higher T_g than PiIF (84 versus 79 °C, respectively). The semi-crystalline nature allowed for SSPC in order to increase the molecular weight (Table 3). First, the polymer was annealed for 1 h at 160 °C. This resulted in a significant increase in the melting enthalpy from 5 to 50 J/g, proving the formation of crystals. Subsequently, the temperature was increased to 185 °C for 48 h. After 48 h, the molecular weight reached an M_n of 38.8 kDa. The polymer showed a T_g of 86 °C (second heating) and a T_m of 217 °C (first heating) which is comparable with the data reported for PEF [44,80]. The polymer did not show a melting transition in the second heating curve, which is attributed to the slow crystallization kinetics for these high-molecular-weight polymers. Earlier work by our group on high-molecular-weight PEF showed similar behaviour [8]. The fact that the addition of 3 mol% isidide in PEF (PE[97]ii[3]F) did not enhance the T_g significantly is not surprising given the relatively low amount of ii. At the same time, the polymer was still semi-crystalline and its molecular weight could be increased by SSPC. A more in depth study on the effect on mechanical properties, crystallization behaviour, barrier properties, and others is out of scope for this study.

Table 2

Molar feed ratio and incorporation ratio of diol:isidide, molecular weight obtained by SEC of the PiIF co-polyesters, and thermal properties determined by DSC of reactor-grade PiIF co-polyesters. Note that a cooling rate of 10 °C/min was used in all DSC measurements unless mentioned otherwise. n.o.: not observed.

Entry	Polymer	Feed ratio	Incorp. ratio	Mn (kDa)	Mw (kDa)	Đ	DSC 1st heating		DSC 2nd heating		ΔH (J/g)	
							Tg (°C)	Tm (°C)	Tg (°C)	Tm (°C)		
1	PiIF	n.a.	n.a.	1.5	4.0	2.8	96	241	30	112	n.o.	n.o.
ethylene glycol												
	PEF	100:0	100:0	33.4	51.9	1.6	80	215	4	79	213	35
	PE[97]ii[3]F	97:3	97:3	11.2	21.6	1.9	83	205	5	84	206	7
	PE[95]ii[5]F	95:5	95:5	18.2	31.6	1.7	83	n.o.	n.o.	80	n.o.	n.o.
	PE[92]ii[8]F	92:8	91:9	27.0	46.5	1.7	91	n.o.	n.o.	85	n.o.	n.o.
	PE[90]ii[10]F	89:11	88:12	25.0	42.8	1.7	95	n.o.	n.o.	92	n.o.	n.o.
	PE[50]ii[50]F	50:50	46:54	16.8	33.7	2.0	128	n.o.	n.o.	116	n.o.	n.o.
	PE[20]ii[80]F	20:80	16:84	6.1	14.6	2.4	134	261	19	135	n.o.	n.o.
	PE[10]ii[90]F	11:89	9:91	4.0	9.8	2.5	119	250	26	126	n.o.	n.o.
	PE[5]ii[95]F	5:95	5:95	2.2	6.6	3.0	105	250	25	118	n.o.	n.o.
1,3-propanediol												
	PPF	100:0	100:0	41.5	62.3	1.5	52	175	8	51	174	34
	PP[95]ii[5]F	95:5	96:4	32.1	62.7	2.0	53	164	1	52	165	1
	PP[90]ii[10]F	89:11	91:9	23.9	48.1	2.0	52	n.o.	n.o.	52	n.o.	n.o.
	PP[50]ii[50]F	51:49	55:45	20.2	36.5	1.8	107	n.o.	n.o.	103	n.o.	n.o.
	PP[20]ii[80]F	18:82	22:78	8.1	16.7	2.0	138	247	7	136	n.o.	n.o.
	PP[10]ii[90]F	12:88	13:87	5.0	14.2	2.8	140	249	18	137	n.o.	n.o.
	PP[5]ii[95]F	5:95	8:92	2.7	7.6	2.8	103	250	26	124	n.o.	n.o.
1,4-butanediol												
	P1,4-BF ^a	100:0	100:0	7.4	17.0	2.3	30	170	56	31	166	52
	P1,4-B[50]ii[50]F ^a	50:50	62:38	9.6	20.2	2.1	77	n.o.	n.o.	78	n.o.	n.o.
	P1,4-B[10]ii[90]F ^a	10:90	14:86	2.2	4.6	2.1	102	n.o.	n.o.	102	n.o.	n.o.
	P1,4-B[5]ii[95]F	5:95	7:93	1.5	4.7	3.1	103	244	22	119	n.o.	n.o.
2,3-butanediol												
	P2,3-BF ^a	100:0	100:0	6.7	14.3	2.1	92	n.o.	n.o.	91	n.o.	n.o.
	P2,3-B[50]ii[50]F ^a	50:50	48:52	3.3	6.7	2.0	99	n.o.	n.o.	96	n.o.	n.o.
	P2,3-B[5]ii[95]F ^a	5:95	6:94	1.5	4.4	2.9	118	235	18	125	n.o.	n.o.

^a DSC cooling rate of 100 °C/min.

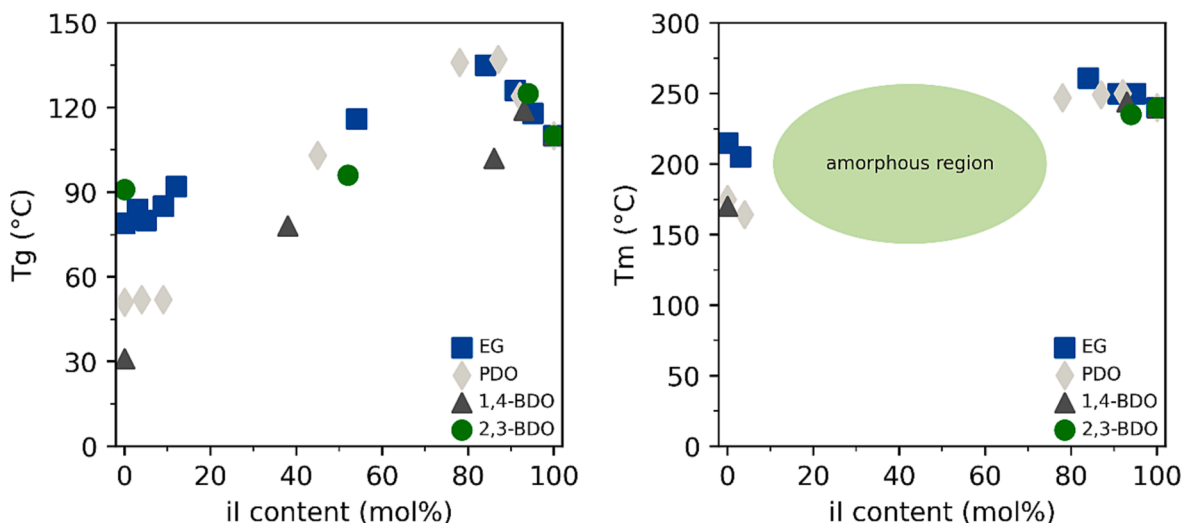


Fig. 6. a) glass transition temperatures (obtained from second dsc heating curves) and b) melting temperatures (obtained from first dsc heating curves) for all piif (co-)polyesters.

4. Conclusions

The melt polycondensation of ii with FDME resulted in low molecular weight PiIF ($M_n < 4$ kDa). Despite their low molecular weight these polyesters have thermal properties well within the “high performance polymers” range. In contrast to PiSF, PiIF was found to be semi-crystalline which is attributed to the symmetrical structure of the ii monomer. Due to the semi-crystalline nature, the molecular weight of PiIF could be significantly enhanced by SSPC yielding a polymer with a T_g of approx. 165 °C and a T_m of approx. 280 °C ($M_n \sim 20$ kDa). This

high melting temperature is too close to the thermal degradation temperature to allow for melt processing. Nevertheless, PiIF provides interesting thermal properties and more research into solution processing of PiIF is required in order to fully unlock its potential.

It was attempted to lower the melting temperature by adding C2-C4 diols as comonomers to PiIF. At relatively high isidide contents (>80 mol%), semi-crystalline polymers were obtained, however, no reduction in melting temperature was observed. Moderate diol comonomer contents (isidide content 5–80 mol%) resulted in fully amorphous polymers, whereas low isidide contents resulted again in semi-crystalline

Table 3

Molecular weight and thermal properties of PE[97]ii[3]F before and after SSPC. A cooling rate of 10 °C/min was used in all DSC measurements. n.o.: not observed, n.d.: not determined.

Entry	T _{SSPC} (°C)	Time (h)	M _n ^a (kDa)	M _w ^a (kDa)	Đ ^b	DSC 1st heating			DSC 2nd heating		
						T _g (°C)	T _m (°C)	ΔH (J/g)	T _g (°C)	T _m (°C)	ΔH (J/g)
1	–	0	11.2	21.6	1.9	83	205	5	84	206	7
2	160	1	10.6	21.9	2.0	85 ^c	202 ^c	50 ^c	n.d.	n.d.	n.d.
3	185	24	26.4	65.4	2.5	n.d.	n.d.	n.d.	n.d.	n.d.	n.d.
4	185	48	38.8	95.9	2.5	91	217	58	86	n.o.	n.o.

^a Obtained from triple detection size exclusion chromatography (SEC), ^b Polydispersity index. ^c Thermal properties obtained by annealing a sample in the DSC and not in the Kugelrohr oven.

polymers (in the case of PE[97]ii[3]F and PP[95]ii[5]F). Due to the semi-crystallinity, the molecular weight of PE[97]ii[3]F could successfully be increased by SSPC, resulting in a polymer with a M_n of 38.8 kDa, a T_g of 86 °C and a T_m of 217 °C. Although the thermal properties are relatively similar to those of PEF, a more in depth study on features such as mechanical properties, crystallization behaviour and barrier properties would be of interest.

CRedit authorship contribution statement

Willem Vogelzang: Conceptualization, Methodology, Validation, Data curation. **Rutger J. I. Knoop:** Conceptualization, Supervision, Methodology, Validation, Data curation. **Daan S. van Es:** Conceptualization, Supervision, Writing – original draft, Writing – review & editing. **Rolf Blaauw:** Conceptualization, Writing – original draft, Writing – review & editing. **Evelien Maaskant:** Conceptualization, Writing – original draft, Writing – review & editing.

Declaration of Competing Interest

The authors declare that they have no known competing financial interests or personal relationships that could have appeared to influence the work reported in this paper.

Data availability

Data will be made available on request.

Acknowledgements

The authors thank Mojgan Heshmat, PhD (Wageningen Food & Biobased Research) for her contribution to the DFT calculations.

This research is part of the Circular and Biobased Performance Materials research programme of Wageningen University and Research and is partly funded by the Dutch Topsector AgriFood and the Dutch Ministry of Agriculture, Nature and Food Quality and by the companies Archer Daniels Midland and Holland Colours.

Appendix A. Supplementary material

Supplementary data to this article can be found online at <https://doi.org/10.1016/j.eurpolymj.2023.112516>.

References

- H.L. Bos, D.S. van Es, P. Harmsen, The renewable future of materials: How to produce our everyday products once we phased out fossil oil and gas, *Wageningen Food & Biobased Research* (2023).
- S. Piotrowski, M. Carus, R. Essel, Nova-Paper #7 on bio-based economy: "Global bioeconomy in the conflict between biomass supply and demand, Full version (2015).
- S. Prasad, et al., Recent advances in the production of 2,5-furandicarboxylic acid from biorenewable resources, *Mater. Sci. Energy Technol.* 6 (2023) 502–521.
- D.J. Aranha, P.R. Gogate, A Review on Green and Efficient Synthesis of 5-Hydroxymethylfurfural (HMF) and 2,5-Furandicarboxylic Acid (FDCA) from Sustainable Biomass, *Ind. Eng. Chem. Res.* 62 (7) (2023) 3053–3078.
- H. Cong, et al., Recent Advances in Catalytic Conversion of Biomass to 2,5-Furandicarboxylic Acid, *Catalysts* 11 (9) (2021) 1113.
- T.P. Kainulainen, et al., Application of Furan-Based Dicarboxylic Acids in Bio-Derived Dimethacrylate Resins, *ACS Appl. Polym. Mater.* 2 (8) (2020) 3215–3225.
- A.F. Sousa, et al., Biobased polyesters and other polymers from 2,5-furandicarboxylic acid: a tribute to furan excellency, *Polym. Chem.* 6 (33) (2015) 5961–5983.
- E. Maaskant, C.V. Aarsen, D.S. van Es, Accelerated weathering of furanoate polyesters: Effect of molecular weight, crystallinity, and time, *J. Appl. Polym. Sci.* 140 (29) (2023) e54062.
- T.P. Kainulainen, et al., Weathering of furan and 2,2'-bifuran polyester and copolyester films, *Polym. Degrad. Stab.* 200 (2022), 109960.
- S.K. Burgess, et al., Water sorption in poly(ethylene furanoate) compared to poly(ethylene terephthalate). Part 1: Equilibrium sorption, *Polymer* 55 (26) (2014) 6861–6869.
- S.K. Burgess, R.M. Krieger, W.J. Koros, Carbon Dioxide Sorption and Transport in Amorphous Poly(ethylene furanoate), *Macromolecules* 48 (7) (2015) 2184–2193.
- S.K. Burgess, et al., Oxygen sorption and transport in amorphous poly(ethylene furanoate), *Polymer* 55 (18) (2014) 4748–4756.
- U. Hoffmann, J. Mueller, DE488602C, Verfahren zur Herstellung wertvoller Produkte aus Sorbit. (1927).
- S. Simar-Mentières, et al., Toxicology and Biodegradability of a Phthalate-Free and Bio-Based Novel Plasticizer, *J. Toxicol.* 2021 (2021) 9970896.
- Y. Chebbi, et al., Synthesis, Characterization, and Biodegradability of Novel Fully Biobased Poly(decamethylene-co-isosorbide 2,5-furandicarboxylate) Copolyesters with Enhanced Mechanical Properties, *ACS Sustain. Chem. Eng.* 7 (5) (2019) 5501–5514.
- Y. Wang, et al., Biodegradability of novel high Tg poly(isosorbide-co-1,6-hexanediol) oxalate polyester in soil and marine environments, *Sci. Total Environ.* 815 (2022), 152781.
- D.H. Weinland, R.-J. van Putten, G.-J.-M. Gruter, Evaluating the commercial application potential of polyesters with 1,4:3,6-dianhydrohexitols (isosorbide, isomannide and isoidide) by reviewing the synthetic challenges in step growth polymerization, *Eur. Polym. J.* 164 (2022).
- J.H. Kamps, et al., Microphase Separation: Enabling Isosorbide-Based Polycarbonates with Improved Property Profile, *Macromolecules* 52 (9) (2019) 3187–3198.
- A.F. Naves, et al., Enzymatic syntheses of unsaturated polyesters based on isosorbide and isomannide, *J. Polym. Sci. Part A: Polym. Chem.* 51 (18) (2013) 3881–3891.
- H. Marubayashi, T. Ushio, S. Nojima, Crystallization of polyesters composed of isohexides and aliphatic dicarboxylic acids: Effects of isohexide stereoisomerism and dicarboxylic acid chain length, *Polym. Degrad. Stab.* 146 (2017) 174–183.
- F. Fenouillot, et al., Polymers from renewable 1,4:3,6-dianhydrohexitols (isosorbide, isomannide and isoidide): A review, *Prog. Polym. Sci.* 35 (5) (2010) 578–622.
- C. Bouyahya, et al., Isosorbide and 2,5-Furandicarboxylic Acid Based (Co) Polyesters: Synthesis, Characterization, and Environmental Degradation, *Polymers* 14 (18) (2022) 3868.
- R. Storbeck, M. Ballauff, Synthesis and thermal analysis of copolyesters deriving from 1,4:3,6-dianhydroisorbitol, ethylene glycol, and terephthalic acid, *J. Appl. Polym. Sci.* 59 (7) (1996) 1199–1202.
- C.D. Papaspyrides, S.N. Vouyiouka, Fundamentals of Solid State Polymerization, *Solid State Polymerization.* (2009) 1–37.
- S. Chang, M.-F. Sheu, S.-M. Chen, Solid-state polymerization of poly(ethylene terephthalate), *J. Appl. Polym. Sci.* 28 (10) (1983) 3289–3300.
- J. Thiem, H. Lüders, Synthesis of polyterephthalates derived from dianhydrohexitols, *Polym. Bull.* 11 (4) (1984) 365–369.
- J. Thiem, H. Lüders, Darstellung und gezielte Polykondensation von Anhydroditol-Bausteinen aus Stärke, *Starch - Stärke* 36 (5) (1984) 170–176.
- R. Storbeck, M. Ballauff, Synthesis and properties of polyesters based on 2,5-furandicarboxylic acid and 1,4:3,6-dianhydrohexitols, *Polymer* 34 (23) (1993) 5003–5006.
- M. Gomes, et al., Synthesis and characterization of poly(2,5-furan dicarboxylate)s based on a variety of diols, *Journal of Polymer Science Part A: Polymer Chemistry* 49 (17) (2011) 3759–3768.

- [30] Parker, D., et al., *Polymers, High-Temperature*, in *Ullmann's Encyclopedia of Industrial Chemistry*.
- [31] Gabara, V., *High-Performance Fibers*, in *Ullmann's Encyclopedia of Industrial Chemistry*, p. 1-22.
- [32] Abts, G., T. Eckel, and R. Wehrmann, *Polycarbonates*, in *Ullmann's Encyclopedia of Industrial Chemistry*, p. 1-18.
- [33] J. Saska, et al., Efficient and Scalable Production of Isoide from Isosorbide, *ACS Sustain. Chem. Eng.* 9 (34) (2021) 11565–11570.
- [34] J. Le Nôtre, J. van Haveren, D.S. van Es, Synthesis of Isoide through Epimerization of Isosorbide using Ruthenium on Carbon, *ChemSusChem* 6 (4) (2013) 693–700.
- [35] D.J. Burke, et al., Ketene-Based Route to rigid Cyclobutanediol Monomers for the Replacement of BPA in High Performance Polyesters, *ACS Macro Lett.* 1 (11) (2012) 1228–1232.
- [36] Eastman Chemical Company. *Selecting Medical Grade Polymers*. [cited 28 april 2023]; Available from: <https://www.tritanmoldit.com/blog/selecting-medical-grade-polymers>.
- [37] H. Shin, et al., Applicability of newly developed PET/bio-based polyester blends for hot-filling bottle, *Food Packag. Shelf Life* 30 (2021), 100757.
- [38] S. Park, et al., PET/Bio-Based Terpolyester Blends with High Dimensional Thermal Stability, *Polymers* 13 (5) (2021) 728.
- [39] A. Little, et al., Effects of Methyl Branching on the Properties and Performance of Furanedioate-Adipate Copolyesters of Bio-Based Secondary Diols, *ACS Sustain. Chem. Eng.* 8 (38) (2020) 14471–14483.
- [40] Z. Terzopoulou, et al., Synthesis and Characterization of Bio-Based Polyesters: Poly(2-methyl-1,3-propylene-2,5-furanoate), Poly(isosorbide-2,5-furanoate), Poly(1,4-cyclohexanedimethylene-2,5-furanoate), *Materials* 10 (7) (2017) 801.
- [41] X. Wang, et al., Synthesis and characterization of poly(isosorbide-co-butylene 2,5-furandicarboxylate) copolyesters, *Eur. Polym. J.* 115 (2019) 70–75.
- [42] S.N. Vouyiouka, E.K. Karakatsani, C.D. Papaspyrides, Solid state polymerization, *Prog. Polym. Sci.* 30 (1) (2005) 10–37.
- [43] D. Wu, et al., Reaction Kinetics and Simulations for Solid-State Polymerization of Poly(ethylene terephthalate), *Macromolecules* 30 (22) (1997) 6737–6742.
- [44] R.J.I. Knoop, et al., High molecular weight poly(ethylene-2,5-furanoate); critical aspects in synthesis and mechanical property determination, *J. Polym. Sci. A Polym. Chem.* 51 (19) (2013) 4191–4199.
- [45] N. Kasmi, et al., Solid-State Polymerization of Poly(ethylene furanoate) Biobased Polyester, I: Effect of Catalyst Type on Molecular Weight Increase, *Polymers* 9 (11) (2017) 607.
- [46] Y.J. Kim, J. Kim, S.-G. Oh, Solid-State Polymerization of Poly(trimethylene terephthalate): Reaction Kinetics and Prepolymer Molecular Weight Effects, *Industrial & Engineering Chemistry Research* 51 (7) (2012) 2904–2912.
- [47] L. Papadopoulos, et al., Towards High Molecular Weight Furan-Based Polyesters: Solid State Polymerization Study of Bio-Based Poly(Propylene Furanoate) and Poly(Butylene Furanoate), *Materials* 13 (21) (2020) 4880.
- [48] I. Shigemoto, et al., A quantum chemical study on the thermal degradation reaction of polyesters, *Polym. Degrad. Stab.* 97 (6) (2012) 941–947.
- [49] P. Sivasamy, et al., The role of β -hydrogen in the degradation of polyesters, *Polym. Degrad. Stab.* 38 (1992) 15–21.
- [50] H. Hopff, A. Lehmann, DE952092 Verfahren zur Herstellung von, Dihydrodifuran. (1956).
- [51] J. Wu, et al., Isohexide derivatives from renewable resources as chiral building blocks, *ChemSusChem* 4 (5) (2011) 599–603.
- [52] J. Wu, et al., Isohexide Dinitriles: A Versatile Family of Renewable Platform Chemicals, *ChemSusChem* 10 (16) (2017) 3202–3211.
- [53] G.P. Dillon, et al., Isosorbide-based cholinesterase inhibitors; replacement of 5-ester groups leading to increased stability, *Bioorg. Med. Chem.* 18 (3) (2010) 1045–1053.
- [54] M. Ralph, S. Ng, K.I. Booker-Milburn, Short Flow-Photochemistry Enabled Synthesis of the Cytotoxic Lactone (+)-Goniofufurone, *Org. Lett.* 18 (5) (2016) 968–971.
- [55] A. Sidduri, M.J. Dresel, S. Knapp, Incorporation of an Isohexide Subunit Improves the Drug-like Properties of Bioactive Compounds, *ACS Med. Chem. Lett.* 14 (2) (2023) 176–182.
- [56] J. Thiem, H. Lüders, Synthese von Oxaprostaglandinen aus 1,4:3,6-Dianhydro-D-sorbit, *Liebigs Ann. Chem.* (1985) 2151–2164.
- [57] P. Villo, et al., Hydroformylation of Olefinic Derivatives of Isosorbide and Isomannide, *The Journal of Organic Chemistry* 81 (17) (2016) 7510–7517.
- [58] C. Berini, et al., Iodoetherification of Isosorbide-Derived Glycols: Access to a Variety of O-Alkyl or O-Aryl Isosorbide Derivatives, *Eur. J. Org. Chem.* 2013 (10) (2013) 1937–1949.
- [59] R.J. Kieber, et al., Cationic copolymerization of isosorbide towards value-added poly(vinyl ethers), *Polym. Chem.* 10 (25) (2019) 3514–3524.
- [60] C. Paolucci, G. Rosini, Approach to a better understanding and modeling of (S)-dihydrofuran-2-yl, (S)-tetrahydrofuran-2-yl-, and furan-2-yl- β -dialkylaminoethanol ligands for enantioselective alkylation, *Tetrahedron Asymmetry* 18 (24) (2007) 2923–2946.
- [61] W.J. McKillip, Chemistry of Furan Polymers, in: *Adhesives From Renewable Resources*, American Chemical Society, 1989, pp. 408–423.
- [62] A. Gandini, M.N. Belgacem, Furans in polymer chemistry, *Prog. Polym. Sci.* 22 (6) (1997) 1203–1379.
- [63] R.-J. van Putten, et al., Hydroxymethylfurfural, A Versatile Platform Chemical Made from Renewable Resources, *Chem. Rev.* 113 (3) (2013) 1499–1597.
- [64] S. Yan, and G, Degradation mechanism and stabilization strategies. *Polymer Degradation and Stability*, Wu, Thermo-induced chain scission and oxidation of isosorbide-based polycarbonates, 2022, p. 202.
- [65] N. Descamps, et al., Isothermal Crystallization Kinetics of Poly(ethylene terephthalate) Copolymerized with Various Amounts of Isosorbide, *Appl. Sci.* 10 (3) (2020) 1046.
- [66] E. Gubbels, et al., Partially renewable copolyesters prepared from acetalized d-glucitol by solid-state modification of poly(butylene terephthalate), *J. Polym. Sci. A Polym. Chem.* 52 (2) (2014) 164–177.
- [67] N. Jacquet, et al., Bio-based alternatives in the synthesis of aliphatic–aromatic polyesters dedicated to biodegradable film applications, *Polymer* 59 (2015) 234–242.
- [68] R. Yamadera, M. Murano, *The determination of randomness in copolyesters by high resolution nuclear magnetic resonance*. *Journal of Polymer Science Part A-1, Polym. Chem.* 5 (9) (1967) 2259–2268.
- [69] Elsevier, *Reaxys*, <https://www.reaxys.com>.
- [70] M. Sokolsky-Papkov, R. Langer, A.J. Domb, Synthesis of aliphatic polyesters by polycondensation using inorganic acid as catalyst, *Polym. Adv. Technol.* 22 (5) (2011) 502–511.
- [71] T.G. Fox, P.J. Flory, Second-Order Transition Temperatures and Related Properties of Polystyrene. I. Influence of Molecular Weight, *J. Appl. Phys.* 21 (6) (1950) 581–591.
- [72] T.G. Fox, P.J. Flory, The glass temperature and related properties of polystyrene. Influence of molecular weight, *J. Polym. Sci.* 14 (75) (1954) 315–319.
- [73] J. Zhu, et al., Poly(butylene 2,5-furan dicarboxylate), a Biobased Alternative to PBT: Synthesis, Physical Properties, and Crystal Structure, *Macromolecules* 46 (3) (2013) 796–804.
- [74] G. Guidotti, et al., Fully Biobased Superpolymers of 2,5-Furandicarboxylic Acid with Different Functional Properties: From Rigid to Flexible, High Performant Packaging Materials, *ACS Sustain. Chem. Eng.* 8 (25) (2020) 9558–9568.
- [75] E. de Jong, et al., Furandicarboxylic Acid (FDCA), A Versatile Building Block for a Very Interesting Class of Polyesters, in: *Biobased Monomers, Polymers, and Materials*, American Chemical Society, 2012, pp. 1–13.
- [76] E. Gubbels, L. Jasinska-Walc, C.E. Koning, Synthesis and characterization of novel renewable polyesters based on 2,5-furandicarboxylic acid and 2,3-butanediol, *J. Polym. Sci. A Polym. Chem.* 51 (4) (2013) 890–898.
- [77] E. Forestier, et al., Understanding of strain-induced crystallization developments scenarios for polyesters: Comparison of poly(ethylene furanoate), PEF, and poly(ethylene terephthalate), *PET. Polymer* 203 (2020), 122755.
- [78] S.K. Burgess, et al., Chain Mobility, Thermal, and Mechanical Properties of Poly(ethylene furanoate) Compared to Poly(ethylene terephthalate), *Macromolecules* 47 (4) (2014) 1383–1391.
- [79] C.F. Araujo, et al., Inside PEF: Chain Conformation and Dynamics in Crystalline and Amorphous Domains, *Macromolecules* 51 (9) (2018) 3515–3526.
- [80] A. Codou, et al., Glass transition dynamics and cooperativity length of poly(ethylene 2,5-furandicarboxylate) compared to poly(ethylene terephthalate), *PCCP* 18 (25) (2016) 16647–16658.